Journal of Applied Fluid Mechanics, Vol. 16, No. 3, pp. 575-589, 2023.
Available online at www.jafmonline.net, ISSN 1735-3572, EISSN 1735-3645.
https://doi.org/10.47176/jafm.16.03.1498

Investigations on Integrated Funnel, Fan and Diffuser Augmented Unique Wind Turbine to Enhance the Wind Speed

K. Ramesh Kumar† and M. Selvaraj

Mechanical Engineering Department, Sri Sivasubramaniya Nadar College of Engineering, Anna University, Chennai, India

†Corresponding Author Email: krameshkumarphd@mech.ssn.edu.in

(Received August 16, 2022; accepted November 11, 2022)

ABSTRACT

Wind energy is an alternative future energy to fossil fuels since it is abundant and green energy. As a result, high performance unique design is proposed that has a diffuser augmented wind turbine including intake funnel with guide vanes, natural fan, straight flow section, exit splitter with air openings and end flange. This proposed design is called as Integrated omni-directional Intake funnel, Natural fan, Straight diffuser, Splitter and Flange (I^2NS^2F) Design. To construct this I^2NS^2F configuration, four distinct wind turbines were developed: a) bare wind turbine, b) wind turbine diffuser design with single rotor turbine, c) bend diffuser, intake funnel, natural fan, splitter and flange and d) I^2NS^2F design. The proposed designs are numerically studied using MATLAB Simulink and Ansys Fluent. These designs are optimized by Random Search Optimization with Supervisory Control and Data Acquisition technique to evaluate the wind velocity and the performance is comparatively estimated. From this analysis, I^2NS^2F design achieves 53m/s of wind velocity at turbine region for 5.5m/s inlet wind and it could be considered as highest wind velocity than other three designs. It is evidently proved and concluded that proposed I^2NS^2F design augments natural wind, resulting in greater green power generation.

Keywords: Increase velocity in omni-directional; Diffuser; Intake hopper; Natural fan; Exit Splitter; MATLAB; CFD.

NOMENCLATURE

ACRIS	Aerodynamic Controllable Roof for INVELOX Structure
ANN	Artificial Neural Network
CFD	Computational Fluid Dynamics
CNN	Convolutional Neural Network
FVM	Finite Volume Method
HAWT	Horizontal Axis Wind Turbine
IEC	international electro technical commission
I^2NS^2F	integrated omni-directional intake funnel, natural fan, straight diffuser, splitter flange design
INVELOX	increased velocity in omni-directional
KE	Kinetic Energy
k-Ɛ	k (turbulent kinetic energy) -Ɛ (dissipation Rate) turbulence model
k-ω	k (turbulent kinetic energy) -ω (specific dissipation rate) turbulence model
LSTM	Long Short-Term Neural Network
NACA	National Advisory Committee for Aeronautics
RANS	Reynolds-averaged Navier-stokes turbulence model
RSO-SCADA	Random Search Optimization with Supervisory Control and Data Acquisition
SST K-ω	Shear Stress Transport K-ω model
TSR	tip speed ratio
VAWT	Vertical Axis Wind Turbine
WT	Wind Turbine

1. INTRODUCTION

Renewable energy resources have had a significant impact on addressing global energy challenges. Wind power, according to the energy conversion system, is the second-largest energy resource that has been developed for long period (Peter and George 2019). Unlike non-renewable resources, the renewable energy source of wind power has provided sustainable growth for the nation due to its benefits as an eco-friendly energy source, non-

radioactive and inexhaustible nature (Trevor 2017). The performance of a wind turbine is actually based on cubic wind velocity and turbine output power, which are proportional to each other. This means that the improvement in wind velocity can make a considerable increase in the output power. VAWT and HAWT are being installed in several nations to produce electricity (Johari *et al.* 2018). Wind turbine with nozzle-diffuser that collects the wind in Omni-directional to increase the wind power by means of speeding up the turbine rotor. This design is named as INVELOX, which stands for increased velocity in Omni-directional (Allaei and Andreopoulos 2014).

INVELOX is a wind turbine integrated with three stages namely wind collector, concentrator and diffuser. In the wind collector section, an intake hopper is placed at the top, which catches the wind from all directions. The next section is a concentrator that collects the wind through a funnel which picks up maximum velocity. The final section is the diffuser, which automatically exhausts excess wind to the ambient. Diffuser composed of three sections such as convergent, venturi and divergent sections. Wind is accelerated through a convergent section to strike the turbine rotor, resulting in less velocity being returned at the final divergent part. The venturi throat section contains a wind turbine that is designed to amplify the wind velocity by generating electrical power. When two turbines are placed in the venturi section then the corresponding secondary rotor consumes a lesser amount of power potential than the primary rotor. INVELOX has a better potential of power output than the single stage when using multi stage turbines (Solanki *et al.* 2017).

Whenever a wind power is testified to accelerate the surrounding wind speed as factor 2 into the INVELOX, then it generates the output power as an increased amount of 4-8 factors. Unlike conventional wind turbines, INVELOX acts better at attaining 6-8 times greater energy at venturi throat section with a wind speed of 11.9 m/s. With this justification, INVELOX generates higher power than the other traditional wind turbines (Patel 2018). Although Omni directional turbines provide superior power output, they are restricted by the accuracy of fluctuating power forecasts. As a result, a dual rotor is assembled in the turbine to reduce the corresponding loss. The output of a dual rotor turbine has greater velocity, which is twice as high as the inlet velocity.

Anbarsooz *et al.* (2017) numerically explained the INVELOX aerodynamic performance by geometrical parameters. The effects of venture diameter, funnel height and inlet area exhibits improved velocity and increased power coefficient for INVELOX design. The aerodynamic performance of wind speed reaches a maximum, then the force around the INVELOX base may not be stable. This instability creates a major problem for the INVELOX structure. As a result, ACRIS was designed to improve structural durability and it can enhance the wind stream efficiency for INVELOX by an aerodynamic controlled roof scheme. This structural design is ideal for increasing system efficiency while limiting the amount of wind that escapes from the system (Golozar *et al.* 2021).

Flanged diffuser based flow mechanism designed using Reynolds-averaged Navier–Stokes equations by Mansour and Meskinkhoda (2014). Owing to this mechanism, power coefficient is achieved in terms of stabilizing the flange height and opening angle of the diffuser under different conditions. For complicated turbine flow, the present work maintains a reasonable prediction of wind power output. The Diffuser Augmented Wind Turbine concept was investigated by Kannan *et al.* (2013) to boost wind velocity and power output.

Four distinct wind turbine designs are created initially and the wind is accelerated towards it. Due to approaching the inlet wind based on wind direction, four concepts are performed individually to evaluate the performance of wind velocity. Using MATLAB Simulink, four designs are generated and their optimized dimensions are determined. After that, the proposed I^2NS^2F Design is simulated in the Ansys tool to get the actual wind velocity and pressure drop. In a less wind speed region, the wind velocity of all four wind turbines is comparatively examined and depicts their result at the conclusion. The research work is organized as follows: section 2 explains the design methodology of four wind turbines, section 4 describes the results and discussions of corresponding wind turbines using two software tools. Finally, the work is concluded in section 5.

2. DESIGN AND OPTIMIZATION METHODOLOGY

In this methodology, four types of wind turbine design are constructed in different ways to reveal the performance of wind velocity. The main ideology of this work is to build up a turbine design in a less wind atmosphere whereas velocity has to be improved at the greater potential. MATLAB Simulink is used to optimize each of the designs. The turbine parameters are optimized using the RSO-SCADA technique. Then, the optimized data with ideal dimensions was gathered from MATLAB Simulink. Lastly, the suggested design is imported into Ansys Fluent to analyze the performance. Figure 1 depicts the workflow of this paper.

2.1 Design

Here, four wind turbine systems are designed and they are listed as follows:

2.1.1 Bare wind turbine design

2.1.2 Diffuser wind turbine design

2.1.3 Bend diffuser design with intake funnel type hopper, natural fan, splitter and flange design

2.1.4 I^2NS^2F design

Let’s make a brief discussion about the design,

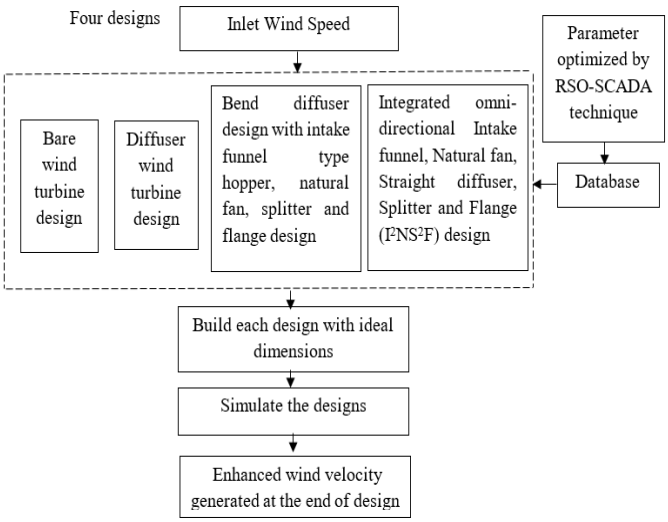

Fig. 1. Design flow diagram of the proposed methodology.

2.1.1 Bare Wind Turbine Design

Wind turbine with three blades is used in this investigation. In case of high winding, the maximum efficiency of HAWT is attenuated (Manwell *et al.* 2009). The conventional wind turbine rotates based on upstream rotor flow and it relatively operates based on Betz limit (De Lellis *et al.* 2018; Sukkiramathi *et al.* 2020). KE is used to accelerate the rotor blade.

The resultant power is expressed as,

$$P_w = \frac{\rho.SA.v^3}{2} \quad (1)$$

According to Betz limit, any wind turbine can operate only a maximum efficiency of 0.59 (Iqbal *et al.* 2020; Lokesharun *et al.* 2019; Goyal *et al.* 2020) and this value is termed as power coefficient (P_c). Generally, the power coefficient should be similar for each category of the turbine. By considering the components of wind turbine devices like gearbox, generator, bearings etc., the available power generated from the wind is defined by,

$$P_{w_{avail}} = \frac{\rho.SA.v^3 P_c}{2} \quad (2)$$

$$SA = \pi R^2 \quad (3)$$

Where, ρ specifies the density, v be its velocity, SA and R implies swept area and its radius respectively.

In this work, a bare wind turbine is built to examine the efficiency. The basic purpose of a wind turbine is simply to convert wind energy into electricity. The main source of input given to the turbine is wind energy, as it is more likely to impact the blades. When wind strikes the blades, then automatically it rotates. The aerodynamic lift force is utilized to generate net torque of rotation on the rotor shaft due to the energy conversion procedure. This rotor shaft produces mechanical power which is transformed into electricity by the generator. The excess of wind is impossible to store for later purposes because wind energy is abundant in nature limit (Rehman *et al.* 2018). Bare design is more suitable to provide stable power generation due to the center position of blade arrangement. But, it is insufficient to generate better power output in a less windy region.

2.1.2 Diffuser Wind Turbine Design

Diffuser wind turbine design accelerates fluid flow in a streamlined curve. Diffuser is a duct-like structure that is composed of three divisions such as convergent, throat/venturi and divergence. The venturi is placed between the convergent and divergent sections. This design is based on several parameters such as converging, venturi and diverging section length along with converging half cone angle and diverging half cone angle section (Jafari and Kosasih 2014).

In the new design, the convergent section is 3479mm in length and divergent of 1200mm. The inlet and outlet diameter of the diffuser is fixed at 2127mm and 2000mm respectively. The throat diameter is 900mm. In addition, convergent section angle and divergent section angle fixed at approximately 9° and 10° respectively.

This diffuser has an augmented cross sectional area that allows the wind to flow across the funnel to reach the turbine section. Without the exit splitter in this design, a greater amount of wind velocity is exhausted through the divergent section. When the wind is driven into this portion, then an automatic pressure drop is created in between the inlet and outlet of the shroud (Ilhan *et al.* 2022). In general, a diffuser encloses the wind turbine while hitting the pressure drop behind the turbine. The pressure drop across the turbine forces the rotor to move in a stream wise direction. With regard to this, more velocity is generated in terms of reducing the pressure drop. This changing criterion of velocity

and pressure is derived by Bernoulli's equation (Khamlaj and Rumpfkeil, 2017).

$$p + \frac{\rho v^2}{2} + \rho a h = k \tag{4}$$

$$\rho = \frac{p \times m}{r \times t} \tag{5}$$

Where, p specifies the static pressure, v and ρ implies the mean velocity and density of airflow, t indicates the temperature of 293K, a, h and k are gravitational acceleration, elevation head center and constant respectively.

The ideology of this approach is to increase the wind velocity from a lower amount of intake wind (Balaji and Gnanambal 2014). But, it does not provide superior wind velocity as an output. The reason is that the diffuser design doesn't have any enforcing medium to pressurize the turbine. Due to this unfair solution, it may degrade the design performance. And also, this diffuser improves the wind velocity without minimizing the exit to rotor area ratio. This in terms, the boundary layer separation arises which significantly lacks the diffuser performance.

2.1.3 Bend Diffuser Design with Intake Funnel Type Hopper, Natural Fan, Splitter and Flange Design

This design is used to offer increased wind velocity as an improved scheme. The following optimum dimensions are considered to construct this design. The diameter and height of the intake hopper are fixed around 2127mm and 2000mm respectively. The height of the divergent turbine is fixed as 1500mm and the outlet diameter of the final section is set at 2691mm. Dual rotor is placed at a specified diameter of around 900mm and the inclination angle deviates from both divergent and convergent sections by around 20°. This design uses lesser wind energy to get greater wind velocity at the venturi section. This design consists of five sections (i) an intake funnel type hopper (ii) a concentrator (iii) a diffuser with bend section, (iv) an exit splitter with opening and (v) an end flange.

Initially, the natural fan at the top of the intake hopper could rotate in response to incoming velocity. The main purpose of a fan is to acquire wind energy from the surface by the way the fan rotates. The additional fan at the hopper section has a tendency to enhance the wind velocity. The next section of the concentrator simply allows the corresponding wind energy through funneling whereas it again improves the wind velocity. In this design, bending guide vanes are utilised to accelerate the wind. Generally, the funnel resembles a non-uniform separation zone and the fact that any solution may eliminate those zones would have improved the system's performance. There are three zones in this diffuser: convergent, venturi and divergent. From the convergent section, the wind flow increases drastically and it strikes the dual rotor at the throat zone. NACA 4418 airfoil profile is used in this experimentation for rotating turbine blades. The advantage of the NACA 4418 blade is to enhance the aerodynamic efficiency by its flow control behaviour. Also, this airfoil has the capability to improve the lift to drag ratio for certain wind directions and speed by varying the airfoil's thickness coefficients suitably (Lou *et al.* 2020). The dual rotor is designed in such a way that it connects the first turbine with the next one. The capacity of the dual rotor is to capture additional energy, resulting in a twofold amount of torque obtained from both the front rotor and rear rotor. Furthermore, the cut-in-speed is also considerably reduced while using the dual rotor. In this duct, the mass flow rate of the second turbine is made a flexible move towards the first turbine in the venturi zone. Additionally, the pressure drop exists through the turbine whereas improving the wind velocity to a greater extent. With this optimized method, the power is generated with higher efficiency at the venturi section. Finally, the divergent section exhausts the remaining wind energy at the outlet environment.

A drawback of this design is that the flow path is oriented horizontally, resulting in considerable head loss and reduced aerodynamic performance. The reason behind this is that as free-flowing wind approaches the turbine, the resistance across the funnel is likely to be maximized, rendering the design ineffective. As a result of this obstacle, the wind outlet velocity may be reduced slightly. In order to improve this difficulty, the straight flow path geometry duct is developed with the vertically positioned venturi section.

2.1.4 I^2NS^2F Design

It is similar to bend diffuser design with intake funnel type hopper and natural fan design, but it is designed in a straight line fluid flow channel. This design generates greater efficiency because of its flow path design.

The diameter and height of the intake hopper are set at 2127mm and 2000mm respectively. Heights of convergent, venturi and divergent sections are made as 3479mm, 70mm and 1200mm respectively. NACA 4418 is installed in a venturi section with a 900mm diameter and an inclination angle 10° and 12° depart from both convergent and divergent sections, respectively. At the bottom layer, exit holes are designed with the intention of exhausting the residual wind velocity. The novel splitter is not forced out the residual velocity. This novel splitter retains the wind speed gradually to produce greater velocity at the venture section of the diffuser since wind speed improvisation is the key factor for power generation.

The size of each hole in the splitter is 90x300mm, with a total of 12 holes and a splitter height of roughly 800mm. The diameter of the divergent end base is almost 2000mm. The purpose of this design is to position the inclined angle at proper proportion and allow the inlet flow towards the turbine to

accelerate the wind velocity, resulting in better aerodynamic performance. The straight flow shape allows the inlet wind to pass through a natural fan and control the turbine's unsteady flow. This beneficial formulation claimed to minimize the pressure coefficient and also enhance the turbine speed due to fluid flow separation on the diffuser plane. Flow separation is formed by adding a flange into the end wall whereas a reduced amount of pressure is exhausted. This intense pressure reduction generates high velocity at the venture zone. So, the design produces a greater amount of wind velocity with high efficiency. The wind turbine uses a dual rotor to rotate the turbine.

2.2 Dual rotor wind turbine design

Two rotors are placed adjacent to each other in this design. Both the rotors are connected with a single shaft to perform operation. Here, wind strikes the small turbine then it easily rotates. Afterwards, the large turbine rotates based on the previous turbine's speed. In this way, high wind velocity is generated at the venturi section. The schematic design of the dual rotor turbine is shown in Fig 2.

Fig. 2. Dual rotor.

Tip speed ratio (Agha *et al.* 2018; Bakırcı and Yılmaz 2018; Bosnar *et al.* 2021) is expressed as,

$$\lambda = \frac{\omega r}{S_w} \tag{6}$$

$$\omega = 2\pi F \tag{7}$$

Where ω specifies turbine's rotational frequency, r and S_w represents the radius of turbine and wind speed respectively. The effect of optimal tip speed ratio due to dual rotor is given by,

$$\lambda_{optimal} = \frac{2\pi.r}{m.S_w} \tag{8}$$

Where m represents the number of rotors, $\frac{r}{S_w}$ denotes the ratio of 1:2. The tip speed ratio is the measure that extracts the greatest amount of power from the wind turbine. Lowering the rotor numbers can higher the turbine rotation. As a result, the dual rotor is used to attain maximum velocity.

3. PARAMETER OPTIMIZATION

In practice, the system dimension plays a critical role in this design process. So, the correct selection of dimensions is necessary for this design to improve the system performance. RSO-SCADA technique is a data optimization system that is employed to optimize geometry parameters of Diffuser type wind turbines. It is directly feasible to optimize several design parameters such as intake hopper, funnel, diffuser, splitter with opening and natural fan respectively. Finally, optimized data is stored into the SCADA system. Figure 3 illustrates the optimization algorithm.

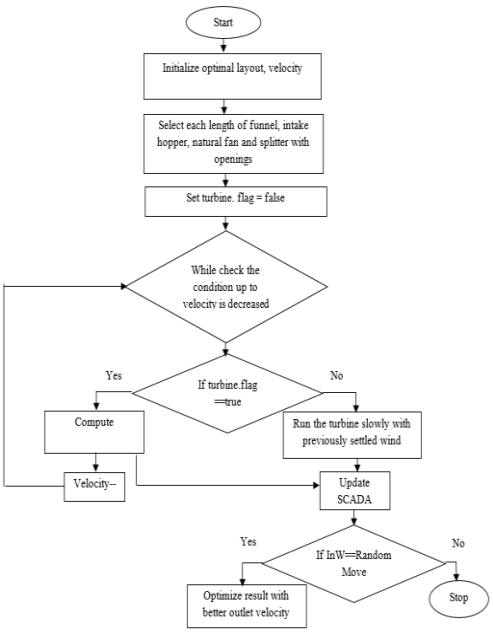

Fig. 3. Design flow diagram of the proposed methodology.

Algorithm:

Step 1: Initialization of optimal design layout (T_0), specifies the optimized parameters of the funnel, intake hopper, natural fan and splitter with openings.

Step 2: Select each length of the funnel, intake hopper, natural fan and splitter with openings

Step 3: Set turbine.flag = false

Step 4: While stop condition if velocity is decreased

Step 5: If (turbine.flag == true)

Compute wind turbine (WT) by taking the inlet wind (InW) along with optimal layout (T_0)

$$WT = InW + T_0 \tag{9}$$

Move to step 9 and connect the optimized random move result to SCADA server

Step 6: Else

Run the turbine slowly with previously settled wind and update the SCADA with obtained wind

Step 7: End if

Step 8: End While

Step 9: If (InW==Random Move)

Get the optimized result with better outlet velocity

Step 10: Else

Stop the iteration process.

Let's make a table for each design with its optimized dimensional value and it is tabulated in Table 1.

Table 1 Optimized parameters of different turbine Design

Critical features of System design	Diffuser design	Bend diffuser design	I^2NS^2F design
Inlet diameter	2127mm	2127mm	2127mm
Height of intake hopper	-	2000mm	2000mm
Convergent height	3479mm	-	3479mm
Diameter of wind turbine	900 mm	900mm	900mm
Divergent height	1200mm	1500mm	1200mm
Inclined angle for convergent section	9°	20°	10°
Inclined angle for divergent section	10°	20°	12°
Outlet diameter	2000mm	2691mm	2000mm

4. Results and Discussions

In the simulation section, four designs of the wind turbine are designed in MATLAB Simulink and the proposed I^2NS^2F design is simulated in Ansys Fluent software. The aforementioned I^2NS^2F design is comparatively analyzed in the two domains and their results as presented below.

4.1 Analytical Studies by MATLAB Simulink

It is a graphical programming tool that is extensively employed to design, simulate and examine the given input and depict the result. In this work, four wind turbine designs are constructed and analyzed the corresponding output by using MATLAB Simulink. While determining the wind turbine outlet velocity, the actual environmental inlet velocity has to be defined. Based on the wind speed, the rotor blade gets rotated and it is shown in Fig. 4.

Fig. 4. Bare wind turbine Design.

4.2 Bare Wind Turbine Design

In this experimental configuration, the inlet velocity of 5.5m/s is applied for the bare design, resulting in a very least wind turbine velocity of just 0.8m/s (Hanna, 2019; Takeyeldein *et al.* 2020). However, this bare design is not suitable for a low circulation wind environment. The simulation result of input wind and its corresponding wind velocity output is shown in Fig 5 and 6. In the graphical plot, the pink line represents the wind direction, yellow line represents the inlet wind and red line denotes the outlet velocity. Based on the wind fluctuation, the inlet wind and its output wind velocity are changed appropriately.

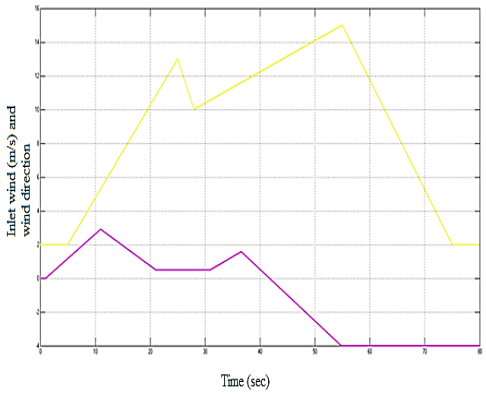

Fig. 5. Inlet wind velocity of bare wind turbine.

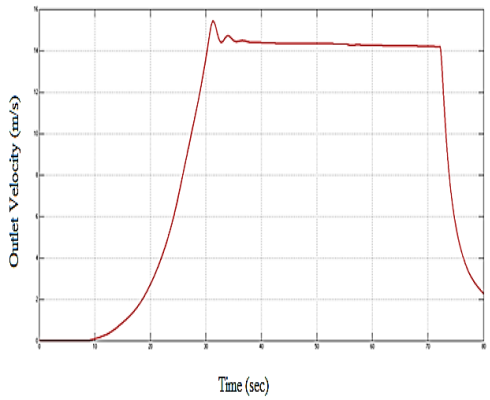

Fig. 6. Outlet wind velocity of bare wind turbine.

4.3 Diffuser Wind Turbine Design

Diffuser design improves the wind velocity in the turbine without connecting the intake hopper, fan and bottom splitter. It analyzes the diffuser behavior using a single rotor, resulting in a higher outlet wind velocity is generated at the venturi section (Takeyeldein *et al.* 2020). A better improvement has been made by extending the length of the divergent section, and this variation is less effective than the bare wind turbine design. At the diffuser entrance, it is notified that the inflow wind carries only lower atmospheric pressure, resulting in improved turbine wind velocity and maximum efficiency. The 3D view of this design, wind input and its output are depicted in Figs 7, 8 and 9.

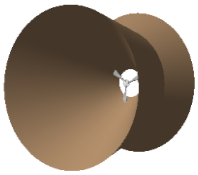

Fig. 7. Diffuser wind turbine design.

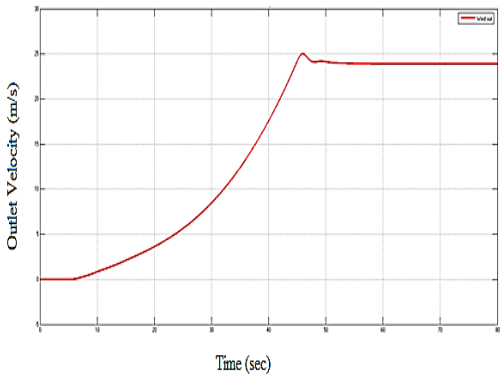

Fig. 8. Inlet wind velocity of bare wind turbine.

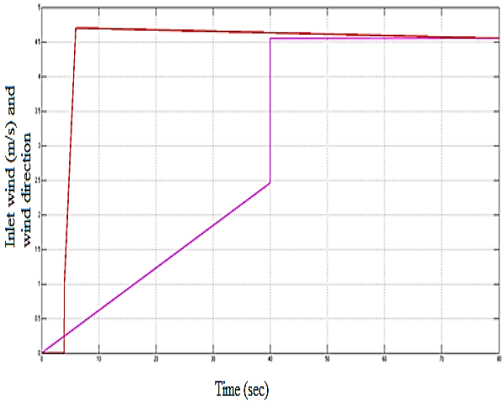

Fig. 9. Outlet wind velocity of bare wind turbine.

Here, the intake wind speed is assumed to be 5.5 m/s, which is a very low wind speed that must be improved. (Nielson *et al.* 2020; Shaterabadi *et al.* 2020; Takeyeldein *et al.* 2020; Zhu *et al.* 2021). Additionally, class IV (Very Low Wind) zones have an annual average wind speed of 6 m/s according to IEC wind class standards. Pink line shows the wind direction and the red line specifies the inlet and outlet wind velocity. Here, the graphical representation of diffuser design shows approximately 24m/s wind velocity is obtained at the throat zone and it is depicted in Fig 8. Pink line shows the wind direction and the red line specifies the inlet and outlet wind velocity. Here, the graphical representation of diffuser design shows approximately 24m/s wind velocity is obtained at the throat zone. The drastic change in wind speed is actually based on wind direction. It is caused by means of moving air conditions or temperature changes. In this design, the rapid improvement in inlet velocity with respect to its corresponding direction can create a slower variation to reach the maximum of 24m/s shown in Fig 9. This diffuser design can't achieve maximum outlet velocity because there is no pressurizing medium to enforce the wind.

4.4 Bend Diffuser Design with Intake Funnel Type Hopper and Natural Fan Design

A 3D view of this design is simulated in MATLAB Simulink and it is revealed in Fig. 10. In order to evaluate the bend section, the flow behavior is constrained by nozzle-diffuser length and the opening angle. Based on its optimized form, the desired output of wind velocity is generated at the throat (venturi). The simulation is analyzed using inlet velocity with respect to its direction and their corresponding velocity is obtained as a result. For the bend diffuser turbine system, the wind flows within a design at varying inlet velocity thus creating a constant improvement in wind velocity due to its bend portion. At the initial stage, the wind direction and its speed become zero. This design can produce a turbine velocity of about 50m/s when an inlet velocity of 5.5m/s is used.

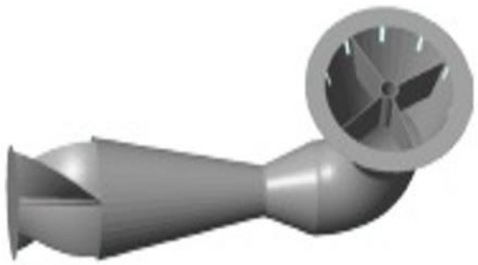

Fig. 10. Bend diffuser design with intake funnel type hopper and natural fan design.

A significant improvement has been observed in this design. The graphical chart reveals the wind input and wind output of the bend diffuser system and it is shown in Figs 11 and 12. After 40 seconds of time duration, both the inlet and its direction remain constant whereas the outlet velocity reaches

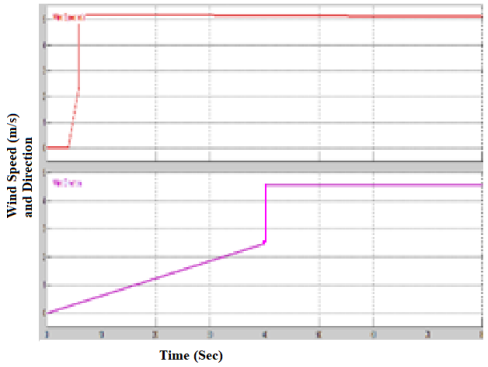

Fig. 11. Inlet velocity changes with regard to its direction.

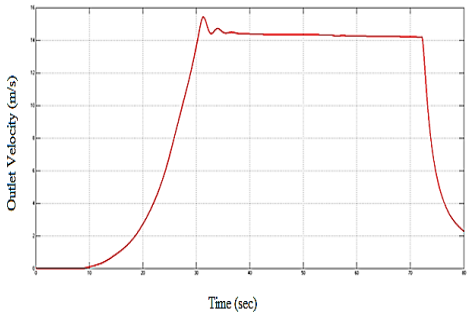

Fig. 12. Outlet wind velocity.

its maximum value. At the diffuser end, some amount of exhaust velocity is eliminated. So, 50m/s of outlet velocity is generated near the turbine zone, while the remaining 9.2m/s of exhaust velocity is liberated and mixed with the environment. In this design, a gradual increase in inlet wind can appropriately increase the wind flow in the venturi section. However, at a certain point, the bend design cannot withstand increased inlet wind speed, resulting in structural instability and deterioration. Figure 11 shows, the inlet wind speed based on direction goes on increasing at 5.5m/s. Figure 12 depicts wind velocity distribution at the turbine rotor zone which is 50m/s. After then, the inlet wind further increases greatly, the design is unable to produce improved outlet velocity as they go on the decreased result. In the exit portion, whatever the inlet wind applied to the design, a small portion of wind is freed through the splitter holes at regular intervals illustrated in Fig 13.

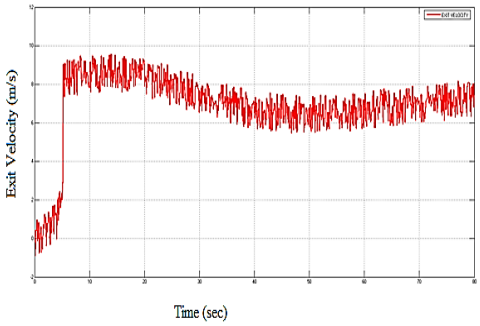

Fig. 13. Exit velocity.

4.5. I^2NS^2F Design

Straight diffuser design with intake funnel type hopper and natural fan design use outlier air and direct it down the funnel to rotate the turbine which is used to generate electricity. Because of its straight fluid flow behavior, the fluid flow inside the design is not collided to resist wind velocity control. A three-dimensional outlook of this design is depicted in Fig. 14, which is modeled in MATLAB Simulink.

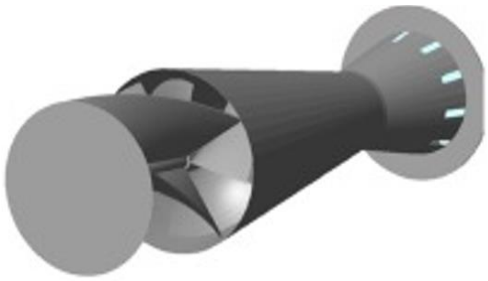

Fig. 14. Straight diffuser design with intake funnel type hopper and natural fan design.

To demonstrate the final design, the input wind is supplied at 5.5m/s. Input wind, output wind velocity and exit wind velocity of I^2NS^2F design as depicted in Figs. 15, 16 and 17. In bend diffuser design, the stability problem occurs in the whole structure which reduces the efficiency. Moreover, velocity head loss of fluid flow was reduced drastically. As a result, the straight design is introduced; here the flow separation across the funnel improvises the turbine area velocity. This means that a constant flow of 5.5 m/s inlet velocity can strike the turbine, while the outlet velocity gradually increases to reach the optimal obtainable outlet velocity of 53m/s at the turbine rotor zone. Regardless of the inlet wind used in the design, a small amount of wind is released via the splitter hole at regular intervals in the exit region.

For each time interval, wind turbine velocity was measured at various input winds. This experimental setup time duration is set as 80 seconds. Because, the turbine fluid flow changes rapidly depending upon the wind direction and the acquired inlet wind. By setting the time, the turbine rotor slowly operate at an initial stage and increased its speed at an appropriate range based on the wind inflow within the turbine (Sessarego *et al.* 2020). During this time frame, the turbine designs are rotated to provide their optimal efficiency of wind velocity. When the turbine velocity of other designs is compared, the bare wind turbine provides the weakest performance. Also, the bend diffuser design was less effective than the I^2NS^2F design, but it offers a significant advantage against bare wind turbines. By considering the inlet wind, the above mentioned I^2NS^2F design is highly feasible for less air circulating environment. When compared to I^2NS^2F design and bend design, the diffuser design gathers a reduced amount of wind velocity and is less than 25 m/s.

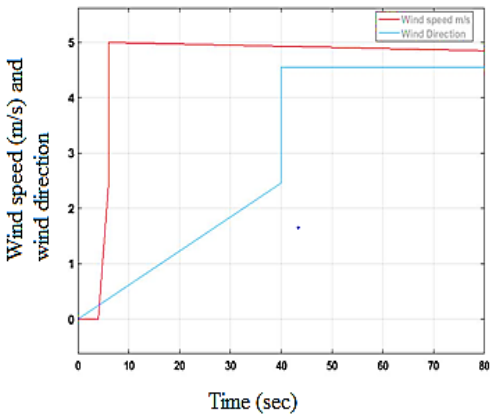

Fig. 15. Wind Speed changes with respect to its direction.

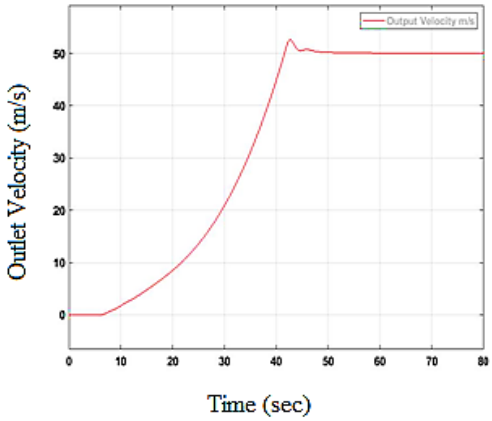

Fig. 16. Outlet wind velocity.

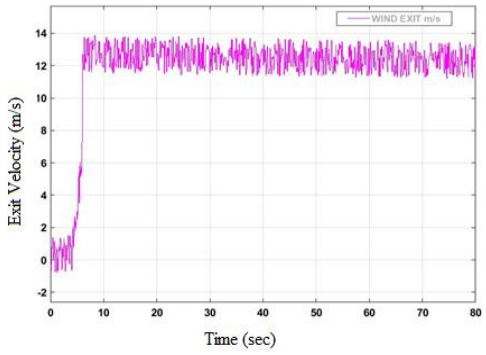

Fig. 17. Exit velocity.

In comparison to the bend, the I^2NS^2F design obtains a maximum velocity of 53m/s. No exhaust velocity is applicable in the first two designs. Also, the diffuser doesn't use a splitter at the divergent end and they resemble as open ended device. As a result, the exhaust region is not applicable in these designs. Both I^2NS^2F design and bend design contains a splitter which is designed at the end of the diffuser with rectangular hole tuned to evacuate the residual quantity of wind in this segment. The Table 2 shows the input, output and exit velocity of different systems.

Table 2 MATLAB Simulink result for different System designs.

S. No	Designs	Inlet wind speed	Gained wind speed	Exit wind speed
1.	Bare wind turbine design	5.5m/s	0.8m/s	-
2.	Diffuser wind turbine design	5.5m/s	24m/s	-
3.	Bend diffuser design with intake funnel type hopper and natural fan design	5.5m/s	50m/s	8.2m/s
4.	I^2NS^2F design	5.5m/s	53m/s	13.5m/s

4.6 Numerical Studies by Ansys Tool

In this study, Ansys Fluent tool is employed which is an FVM approach tool to solve the pressure and velocity distribution. Also, CFX uses the vertex-centered technique. Fluent employs cell-centered techniques, which have more DOF but few fluxes per unit of time. The time-averaged continuity and time-averaged momentum equations are considered as a Governing equation. The k-Ɛ turbulence model proposed by Launder and Spalding, is for high Reynolds number and negligible molecular viscosity and k-ω model proposed by Wilcox, is for less compressibility and Reynolds number and shear flow spreading (Aresti *et al.* 2013). Based on the flow physics, RANS SST K-ω turbulence model was used in this study (Kosasih and Hudin 2016; Amiri *et al.* 2019; Sogukpinar 2020; Mirfazli *et al.* 2019; Alanis *et al.* 2021). Because, this model solves velocity nearby wall zone as well as far away region, which is a hybrid of k-ω and k-Ɛ turbulence model. Also, it predicts the capability of aerodynamic properties like boundary layer separation and pressure drop.

The optimized output with its perfect dimension is simulated using the Ansys tool, in this section. Here, the final design is modeled in the SolidWorks CAD tool and saved the file in Parasolid (X_T) format. In the Ansys workbench, the given straight design is constructed in a possible way to prepare geometry and mesh generation. A schematic view of I^2NS^2F design and its dimension is revealed in Figs 18 and 19. Here, the air was modeled as an ideal gas at room temperature. It is an essential tool for discretizing the computational domain based on mapped meshing. It is fine and smooth in several regions away from the duct. Using the edge sizing method, an appropriate mesh size of 120 is chosen during simulation. The boundary conditions are set up to reflect the condition of the design and fixed inlet free stream velocity applied.

Fig. 18. CAD Geometry of I²NS²F design.

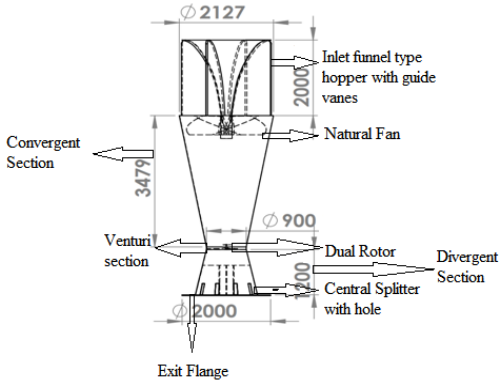

Fig. 19. I²NS²F Critical dimensions.

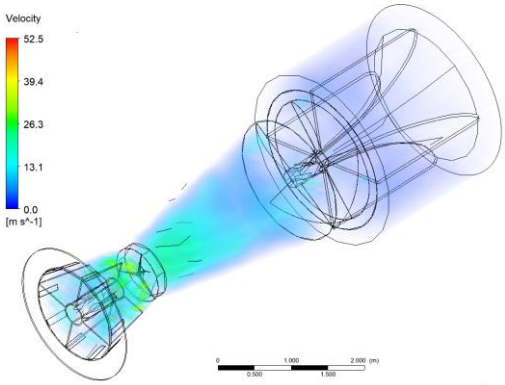

Fig. 20. Velocity variation of I²NS²F design.

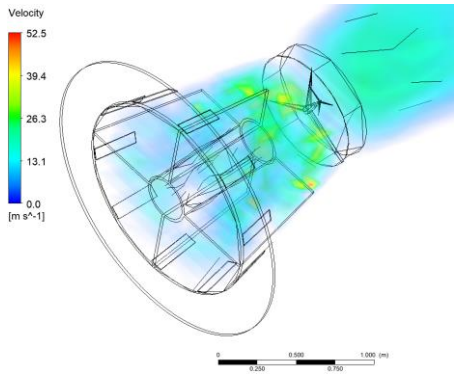

Fig. 21. Turbine area velocity contour of I²NS²F design.

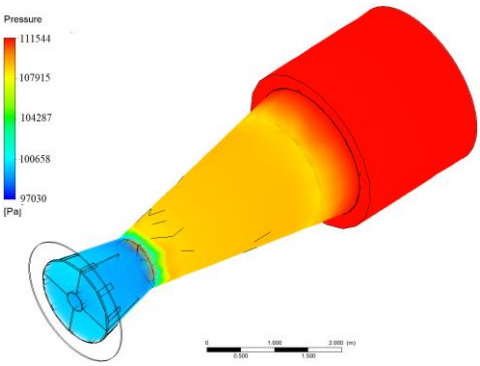

Fig. 22. Pressure distribution of I²NS²F design.

It is evident that increasing diffuser wall length leads to achieving increased wind velocity. To perform this, the diffuser setup is raised to almost 6679mm. More specifically, the improvement in the throat section reaches maximum velocity by means of raising the length and intake mass flow rate. Figs 20, 21and 22 illustrate the results of wind velocity, turbine area velocity, exit velocity and pressure distribution. The above contours are evaluated using the inlet wind stream velocity of 5.5m/s. Actually, 1.375 m/s of inlet wind velocity is applied in all four directions of the intake hopper. The simulation result of the I²NS²F design specifies the maximum wind velocity of 52.5m/s as shown in Fig 20. The boundary layer separation of fluid flow at natural fan and venture zone of the turbine at this velocity is less which makes negligible energy loss. So, available energy is used to run the turbine. At the initial hopper section, the inlet wind is almost very low, but as it progresses to the following section of convergent, it improves drastically and approaches a speed of approximately 32.6m/s. Finally, the wind reaches the turbine zone, the wind velocity exceeds the maximum value and then reduces to a minimum value at the divergent section. The simulation result of turbine zone velocity is exhibited in Fig. 21. The wind velocity achieves 52.5m/s, with an exit velocity of 28.5m/s. This enhanced velocity should maintain the turbine to act better in a low-windy environment. It is caused by its optimized geometry dimensions and arrangement of components. In this case, the turbine obtains an improved outlet velocity of 52.5m/s, which is regarded as the best optimum value of a straight diffuser design. This improvement is caused due to more compact layout of the convergent outlet area. The smaller diameter of the convergence, the faster the wind velocity and so they extract more energy due to avoiding the kinetic energy loss. Few amounts of fluid flow from the backside of the turbine are exhausted and escaped via the splitter holes. Here, 28.5m/s of exit velocity is escaped from the divergent end.

Pressure drop exists in the inlet hopper, convergent, venture and divergent sections. The venturi regulates the wind speed, which results in pressure drops occurring at the end. The convergence starts to move the fluid from a larger area to a narrower area. To accelerate the speed of air, this system

obeys mass conservation laws. As the result, the turbine rotates faster to enhance the fluid speed by reducing the pressure. The ambient pressure enters the intake hopper at 111544Pa due to the usual environmental condition, and it gradually drops to 97030Pa at the rear of the wind turbine, as shown in Fig. 22. The increase in velocity owing to reduce the pressure due to considerable flow separation over the trailing edge of the rotor, wake rotation and imposed fluid flow. A minimum pressure of 97030Pa was found towards the rear of the turbine. The pressure drop witnessed from intake hopper to diffuser end gradually.

While compared to other designs, the I^2NS^2F design achieves maximum velocity at a lesser wind inlet and it has been validated in CFD numerical simulation using Standard Ansys Program.

Velocity variation along the linear wind flow path distance of the proposed I^2NS^2F design as a bar chart is revealed in Fig 23. The maximum wind velocity occurred is 52.5m/s where the turbine rotor is installed and dropped gradually until the end of the system. The largest pressure drop is found at the venturi section of the wind turbine system due to less area ratio and system exit due to atmospheric conditions at the end of the flow path. This pressure drop permits the velocity flow to rise as it passes through this zone, according to Bernoulli's principle and the continuity equation. Also, a pressure drop occurred behind the end flange of this design due to vortex generation. The graphical pressure distribution bar chart for the suggested I^2NS^2F design is shown in Fig 24.

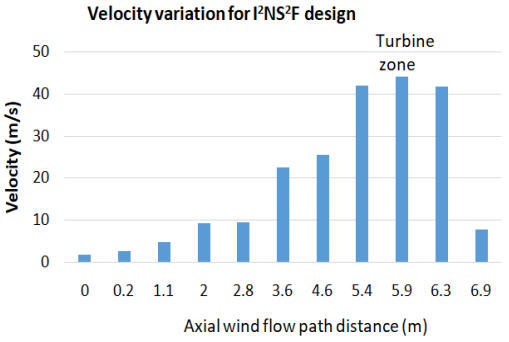

Fig. 23. Velocity variation of I^2NS^2F design along the Flowpath.

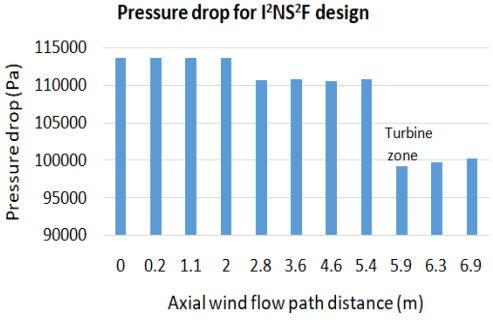

Fig. 24. Pressure drop along the axial wind flow distance for I^2NS^2F design.

Finally, numerical and analytical results are comparatively investigated and the outcome is shown in Fig 25, which illustrates I^2NS^2F design output in both MATLAB Simulink and Ansys tool. It uses 5.5 m/s of inlet wind to reach a maximum velocity of 53m/s and 52.5m/s at turbine rotor installation as output in MATLAB Simulink and Ansys Fluent tool respectively. By concluding the investigation with its perfect optimized dimension, both methodologies produce 87.07% of equivalent output. Based on this result, it is possible to conclude that the I^2NS^2F design is better suited to low windy class zones 3 and 4 (IEC Wind class).

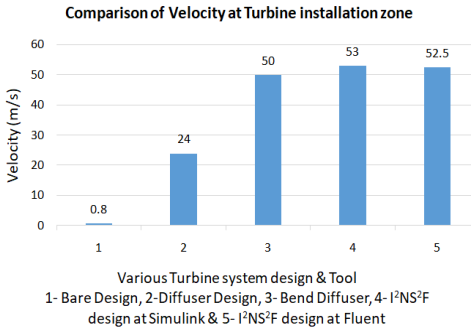

Fig. 25. Comparison of output velocity in MATLAB Simulink and Ansys Fluent Tool.

4.7 Verification of Design Consistency

The input free stream wind velocity was set at 5m/s, 5.5m/s and 6m/s for the I^2NS^2F design, and the corresponding enhanced velocity at various critical locations was taken to evaluate the design consistency in Ansys. The velocity along flow path for various input velocity is shown in Fig 26. Furthermore, this design increased the wind speed at the turbine entry location from 4.6 m/s, which is classified as very low wind to 22.2 m/s.

The velocity enhancement agrees with the cross-section area of the proposed design, depicted in Fig. 27. The pressure drop chart plotted for various input free stream wind velocities of 5m/s, 5.5m/s and 6m/s are revealed in Fig 28. The pressure difference in each region is caused by the difference in cross-section area.

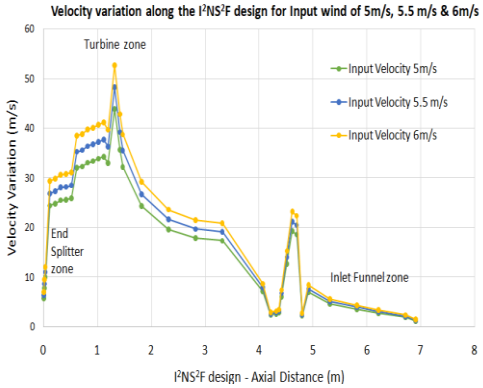

Fig. 26. Velocity variations for I^2NS^2F design for the input wind speed of 5m/s, 5.5m/s & 6m/s.

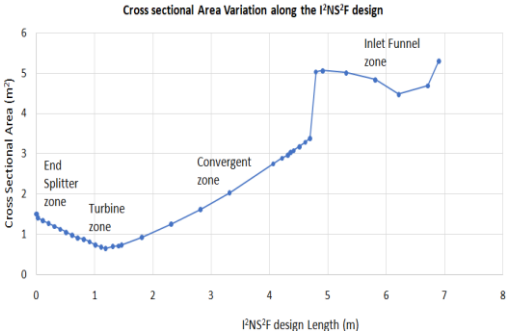

Fig. 27. Cross section variation along the axial length.

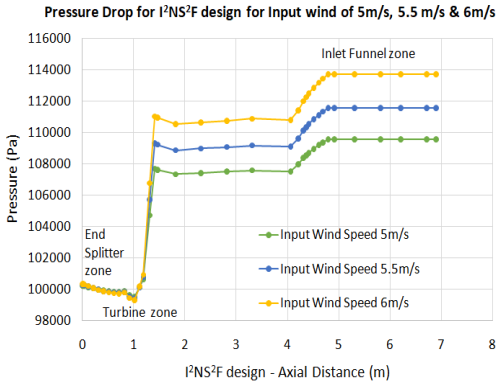

Fig. 28. Pressure drop for I²NS²F design for the input wind speed of 5m/s, 5.5m/s & 6m/s.

4.8 Power Estimation

Wind turbine power generation can be enhanced by improving mass flow rate and the pressure drop across the turbine. In this I²NS²F design both rules are captured efficiently to achieve the maximum power rate of 1917W for the wind speed of 5.5m/s at Turbine installation zone, by considering E_w = 50% E_T = 40% and E_G = 65%. In general, the productivity of wind power is lowered due to losses such as profile losses, end losses, whirlpool losses, blade number losses, frictional losses in gears, and electrical resistance losses in the alternator, among others and it is estimated as below (Çetin *et al.* 2005; Ragheb and Ragheb 2011).

$$P = \frac{1}{2}\rho \times A \times E_w \times E_T \times E_G \times v^3 \qquad (10)$$

Where, Wind power is represented by p, wind density is defined as ρ, swept area is denoted as A, Whirlpool losses as E_w, Turbine efficiency rating as E_T, Generator efficiency rating is defined as E_G, and velocity of the wind is defined as v. The wind power generation along the various location of I²NS²F design is plotted for various input free stream wind velocities of 5m/s, 5.5m/s and 6m/s are depicted in Fig 29.

I²NS²F system can be erected even in wind class zones 3 and 4 (IEC Wind class), where the average wind speed is 7.5 m/s and 6 m/s, respectively, it can produce substantially more energy than conventional wind turbines.

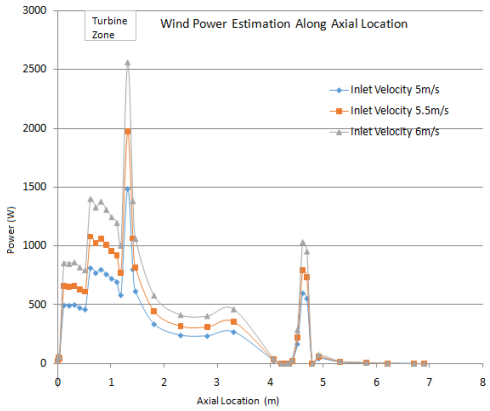

Fig. 29. Wind power production in I²NS²F design for the various input wind speed.

4.9 Velocity and Power Prediction

Deep learning methodology is used to forecast wind velocity and power prediction for various input wind stream. This deep learning models works mainly on data processing, developing the prediction model, and training and estimation from the prediction model such as ANN, LSTM, CNN algorithm. (Nielson *et al.* 2020; Zhu *et al.* 2021).

In Python programming, a deep learning prediction model framework can be developed to estimate the wind speed and energy. It is simple to use and it can be employed for rapid prototyping and inventive design modifications.

4.10 Result Comparison with Previous Studies

Speed Ratio for I²NS²F design can be estimated by continuity equation at inlet and venturi terminals. So, Speed ratio is expressed as,

$$SR = \frac{V_{inlet}}{V_{venturi}} \qquad (11)$$

$$SR = \frac{4.\,D_{in} \times H_{in}}{\pi \times D_{ve}^{\,2}} \qquad (12)$$

Where, Wind inlet diameter, Height of Guide vanes and Venturi diameter are represented by D_{in}, H_{in} and D_{ve} respectively. Therefore, I²NS²F design achieved SR of 6.7 as per theoretical calculation. But, simulation studies show that speed ratio as 9.5. It is about 41.7% error. The investigations on duct-based design, inlet wind speed, and throat wind speed were summarized in Table 3.

5. CONCLUSIONS

This research manuscript describes the evolution of unique I²NS²F Design, which incorporates four wind turbine concepts to augment wind speed in

Table 3 List of existing studies on INVELOX Wind turbine System.

S. No	Design	Inlet wind Speed	Throat wind Speed	Published Details
1.	INVELOX Multi stage wind turbine with propeller fan model	10.4 m/s	45.5 m/s	Gohar *et al.* (2019)
2.	Wind Funnel Concentrator system	4.7 m/s	17.12m/s (Simulation) 10.87m/s (Experiments) Relative Error 39%	Akour and Bataineh (2019)
3.	Wind Tunnel Testing of Funnel Based Wind Energy Harvesting System	7.8 m/s	20.7 m/s	Nallapaneni *et al.* (2015)
4.	Improved INVELOXwind shield model	6.7 m/s	15.6 m/s	Ding and Guo (2020)
5.	DAWT with End splitter	4m/s	8.6m/s (SR=2.2)	Thangavelu *et al.* (2020)
6.	INVELOX with the new curtain design	6.7 m/s	13.1m/s (SR=1.95)	Anbarsooz *et al.* (2019).

low wind zones. The proposed designs are numerically studied using MATLAB Simulink and Ansys Fluent and its wind velocity and pressure distribution are determined. The bare wind turbine performs the least compared to the other three designs, based on the final outcome. In order to provide greater wind velocity in less wind zones, the I^2NS^2F design works well. The result shows the proposed design reaches the maximum of approximately 52.5m/s of wind turbine velocity for 5.5m/s intake free wind stream at the turbine rotor zone. The corresponding output is analytically evaluated in MATLAB Simulink and is numerically simulated in the Ansys Fluent tool and the results are compared. Moreover, for various input streams, design consistency for the proposed design was validated.

Due to the following design elements, the proposed I^2NS^2F design has high efficiency to increase wind velocity and reduce pressure drop.

- Hopper with inlet fan sucks Omni-directional wind from all four directions.
- Natural fan collects the inlet wind and moves it through the convergent section.
- Based on the optimized dimension and proper inclined angle of 10° and 12° at convergent and divergent section prevents sudden change in wind flow path. It will prohibit the loss of kinetic energy and maintain forward motion of the wind.
- In between the convergent and divergent sections, the venture used a dual rotor to rotate the turbine which is highly possible to enhance the aerodynamic efficiency.
- Lastly, the end splitter with the opening is placed at the divergent section that allows the turbine to exit the residual wind to the ambient.

As a result, I^2NS^2F wind turbine system reached a venturi section wind speed of 52.5 m/s with that speed ratio as 9.5. There is a 41.7% deviation compared to the theoretical prediction. It can be stated that proposed I^2NS^2F wind turbine for low windy region (IEC Wind class zones 3 and 4) is developed to harness the wind power environment friendly, less noisy, economically viable and uninterrupted manner.

Despite the promising outcomes of I^2NS^2F design, further research on deep learning model to predict the velocity along the flow path of the for various input wind stream and wind tunnel testing for physical prototype is still necessary.

ACKNOWLEDGMENTS

The research illustrated in this paper was performed in Sri Sivasubramaniya Nadar College of Engineering, An Autonomous Institution, Anna University, Chennai, India.

REFERENCES

Agha, A., H. N. Chaudhry and F. Wang (2018). Diffuser augmented wind turbine (DAWT) technologies: a review. International *Journal of Renewable Energy Research* 8(3), 1369-1385.

Akour, S. N. and H. O. Bataineh (2019). Design considerations of wind funnel concentrator for low wind speed regions. *AIMS Energy* 7(6), 728-742.

Alanis, A., J. A. Franco, S. Piedra and J. C. Jauregui (2021). A novel high performance diffuser design for small DAWT's by using a blunt trailing edge airfoil. *Wind and Structures* 32(1), 47-53.

Allaei, D. and Y. Andreopoulos (2014). INVELOX: Description of a new concept in wind power and its performance evaluation. *Energy* 69, 336-344.

Amiri, M., M. Kahrom and A. R. Teymourtash (2019). Aerodynamic Analysis of a Three-Bladed Pivoted Savonius Wind Turbine: Wind Tunnel Testing and Numerical Simulation. *Journal of Applied Fluid Mechanics* 12(3), 819-829.

Anbarsooz, M., H. Mohammad Sadegh and B. Moetakef-Imani (2017). Numerical study on the geometrical parameters affecting the aerodynamic performance of INVELOX. *IET Renewable Power Generation* 11(6), 791-798.

Anbarsooz, M., M. Amiri and I. Rashidi (2019). A novel curtain design to enhance the aerodynamic performance of invelox: A steady-RANS numerical simulation. *Energy* 168, 207-221.

Aresti, L., M. Tutar, Y. Chen and R. K. Calay (2013). Computational study of a small scale vertical axis wind turbine (VAWT): comparative performance of various turbulence models. *Wind and Structures* 17(6), 647-670.

Bakırcı, M. and S. Yılmaz (2018). Theoretical and computational investigations of the optimal tip-speed ratio of horizontal-axis wind turbines. *Engineering Science and Technology, an International Journal* 21(6), 1128-1142.

Balaji, B. and I. Gnanambal (2014). Wind power generator using horizontal axis wind turbine with convergent nozzle. *Journal of Scientific & Industrial Research* 73, 375-380.

Bosnar, D., H. Kozmar, S. Pospisil and M. Machacek (2021). Thrust force and base bending moment acting on a horizontal axis wind turbine with a high tip speed ratio at high yaw angles. *Wind and Structures* 32(5), 471-485.

Çetin, N. S., M. A. Yurdusev, R. Ata and A. Özdamar (2005). Assessment of optimum tip speed ratio of wind turbines. *Mathematical and Computational Applications* 10(1), 147-154.

De Lellis, M., R. Reginatto, R. Saraiva and A. Trofino (2018). The Betz limit applied to airborne wind energy. *Renewable Energy* 127, 32-40.

Ding, L. and T. Guo (2020). Numerical study on the power efficiency and flow characteristics of a new type of wind energy collection device. *Applied Sciences* 10(21), 7438.

Gohar, G. A., T. Manzoor, A. Ahmad, Z. Hameed, F. Saleem, I. Ahmad, A. Sattar and A. Arshad (2019). Design and comparative analysis of an INVELOX wind power generation system for multiple wind turbines through computational fluid dynamics. *Advances in Mechanical Engineering* 11(4), 1687814019831475.

Golozar, A., F. A. Shirazi, S. Siahpour, F. N. Khakiani and K. Gaemi Osguei (2021). A novel aerodynamic controllable roof for improving performance of INVELOX wind delivery system. *Wind Engineering* 45(3), 477-490.

Goyal, S., S. K. Maurya, S. Kumar and D. Agarwal (2020). A Consolidation Review of Major Wind Turbine Models in Global Market. In *International Conference on Power Electronics & IoT Applications in Renewable Energy and its Control* (PARC), IEEE.

Hanna, S. (2019). *Introducing INVELOX Technology to Generate Energy Using Wind and Wind Turbines by Retrofitting Traditional Wind Turbines* Master's thesis. California State University, Sacramento.

İlhan, A. K. I. N., S. Tumse, M. Oguz Tasci, M. E. H. M. E. T. Bilgili and B. Sahin (2022). Particle image velocimetry investigation of the flow for the curved type wind turbine shroud. *Journal of Applied Fluid Mechanics* 15(2), 373-385.

Iqbal, A., D. Ying, A. Saleem, M. A. Hayat and K. Mehmood (2020). Efficacious pitch angle control of variable-speed wind turbine using fuzzy based predictive controller. *Energy Reports* 6, 423-427.

Jafari, S. A. and B. Kosasih (2014). Analysis of the power augmentation mechanisms of diffuser shrouded micro wind turbine with computational fluid dynamics simulations. *Wind and Structures* 19(2), 199-217.

Johari, M. K., M. Jalil and M. F. M. Shariff (2018). Comparison of horizontal axis wind turbine (HAWT) and vertical axis wind turbine (VAWT). International *Journal of Engineering and Technology* 7(4.13), 74-80.

Kannan, T. S., S. A. Mutasher and Y. K. Lau (2013). Design and flow velocity simulation of diffuser augmented wind turbine using CFD. *Journal of Engineering Science and Technology* 8(4), 372-384.

Khamlaj, T. A. and M. P. Rumpfkeil (2017). Theoretical analysis of shrouded horizontal axis wind turbines. *Energies* 10(1), 38.

Kosasih, B. and H. S. Hudin (2016). Influence of inflow turbulence intensity on the performance of bare and diffuser-augmented micro wind turbine model. *Renewable Energy* 87, 154-167.

Lokesharun, D., S. Rameshkumar, B. S. Navaneeth and R. Kirubakaran (2019). Design and Analysis of Diffuser Augmented Wind Turbine using CFD. *International Journal of Mechanical and Industrial Technology* 7 (1), 1-13.

Lou, B., Z. Huang, S. Ye and G. Wang (2020). Experimental and numerical studies on aerodynamic control of NACA 4418 airfoil with a rotating cylinder. *Journal of Vibration Engineering & Technologies* 8(1), 141-148.

Mansour, K. and P. Meskinkhoda (2014). Computational analysis of flow fields around flanged diffusers. *Journal of Wind Engineering and Industrial Aerodynamics* 124, 109-120.

Manwell J. F., J. G. McGowan and A. L. Rogers (2009). *Wind Energy Explained Theory, Design and Application*. Second Edition. ISBN 978-0-470-01500-1.

Mirfazli, S. K., M. H. Giahi and A. J. Dehkordi (2019). Numerical optimization of a vertical axis wind turbine: case study at TMU campus. *Wind and Structures* 28(3), 191-201.

Nallapaneni M. K., M. S. P Subathrab and O. D. Cota (2015). Design and Wind Tunnel Testing of Funnel Based Wind Energy Harvesting System. *Elsevier Procedia Technology* 21 (2015) 33 – 40.

Nielson, J., K. Bhaganagar, R. Meka and A. Alaeddini (2020). Using atmospheric inputs for Artificial Neural Networks to improve wind turbine power prediction. *Energy* 190, 116273.

Patel S. N. (2018). Numerical simulation of flow through INVELOX wind turbine system. *International Journal of Renewable Energy Research* 8, 291–301.

Peter, E. and X. George (2019). Examining the trends of 35 years growth of key wind turbine components. *Energy for Sustainable Development* 50, 18–26.

Ragheb, M. and A. M. Ragheb (2011). Wind turbines theory-the betz equation and optimal rotor tip speed ratio. *Fundamental and Advanced Topics in Wind Power* 1(1), 19-38.

Rehman, S., M. M. Alam, L. M. Alhems and M. M. Rafique (2018). Horizontal axis wind turbine blade design methodologies for efficiency enhancement-A review. *Energies* 11(3), 506.

Sessarego, M., J. Feng, N. Ramos-García and S. G. Horcas (2020). Design optimization of a curved wind turbine blade using neural networks and an aero-elastic vortex method under turbulent inflow. *Renewable Energy* 146, 1524-1535.

Shaterabadi, M., M. A. Jirdehi, N. Amiri and S. Omidi (2020). Enhancement the economical and environmental aspects of plus-zero energy buildings integrated with INVELOX turbines. *Renewable Energy* 153, 1355-1367.

Sogukpinar, H. (2020). Numerical investigation of influence of diverse winglet configuration on induced drag. Iranian Journal of Science and Technology. *Transactions of Mechanical Engineering* 44(1), 203-215.

Solanki A. L., B. D. Kayasth and H. Bhatt (2017). Design modification & analysis for venturi section of INVELOX system to maximize power using multiple wind turbine. *International Journal for Innovative Research in Science & Technology* 3, 125-127.

Sukkiramathi, K., R. Rajkumar and C.V. Seshaiah (2020). Evaluation of wind power potential for selecting suitable wind turbine. *Wind and Structures* 31(4), 311-319.

Takeyeldein, M. M., T. M. Lazim, I. S. Ishak, N. A. R. Nik Mohd and E. A. Ali (2020). Wind lens performance investigation at low wind speed. *Evergreen* 7(4), 481-8.

Thangavelu, S. K., T. G. L. Wan and C. Piraiarasi (2020). Flow simulations of modified diffuser augmented wind turbine. *In IOP Conference Series: Materials Science and Engineering*, IOP Publishing.

Trevor, M. L. (2017). *Wind Energy Engineering: A Handbook for Onshore and Offshore Wind Turbines*, Chapter 1, ISBN 978-0-12-809451-8.

Zhu, X., R. Liu, Y. Chen, X. Gao, Y. Wang and Z. Xu (2021). Wind speed behaviors feather analysis and its utilization on wind speed prediction using 3D-CNN. *Energy* 236, 121523.